Minimum-Delay Routing for Integrated Aeronautical *Ad Hoc* Networks Relying on Real Flight Data in the North-Atlantic Region

Jingjing Cui, *Member, IEEE*, Dong Liu, *Member, IEEE*, Jiankang Zhang, *Member, IEEE*, Halil Yetgin, *Member, IEEE*, Soon Xin Ng, *Senior Member, IEEE*, Robert G Maunder, *Senior Member, IEEE*, and Lajos Hanzo, *Fellow, IEEE*

***Abstract*—Relying on multi-hop communication techniques, aeronautical *ad hoc* networks (AANETs) seamlessly integrate ground base stations (BSs) and satellites into aircraft communications for enhancing the on-demand connectivity of planes in the air. The goal of the paper is to assess the performance of the classic shortest-path routing algorithm in the context of the real flight data collected in the North-Atlantic Region. Specifically, in this integrated AANET context we investigate the shortest-path routing problem with the objective of minimizing the total delay of the in-flight connection from the ground BS subject to certain minimum-rate constraints for all selected links in support of low-latency and high-speed services. Inspired by the best-first search and priority queue concepts, we model the problem formulated by a weighted digraph and find the optimal route based on the shortest-path algorithm. Our simulation results demonstrate that aircraft-aided multi-hop communications are capable of reducing the total delay of satellite communications, when relying on real historical flight data.**

I. Introduction

With the proliferation of Internet services and applications, it is desirable to provide high-speed broadband access during flights above the clouds. As mentioned in Airbus' Global Market Forecast (GMF) [1], passenger traffic growth would increase by about 50% by the year 2038 and air traffic as a whole will grow at 4.3% annually over the next 20 years. This forecast further inspires the wide roll-out of in-flight Internet access in aeronautical systems. However, since aircraft fly at a high speed, it is challenging to integrate conventional terrestrial communication solutions into aeronautical systems.

Existing aircraft connectivity solutions can be broadly categorized into two classes [2], [3]: satellite to aircraft communication (S2AC) and direct aircraft to ground communication (DA2GC). At the time of writing in-flight connectivity of aircraft mainly depends on satellites. In particular, often geostationary Earth orbit (GEO) satellites are used for providing on-board connectivity for aircraft as a benefit of their near-global coverage, supporting longer-lasting connections than DA2GC and aircraft-to-aircraft communication (A2AC) without the need for handovers between GEO satellites. For example, GoGo has more than 1,000 aircraft that are equipped with in-flight satellite connectivity, relying on the Gogo 2Ku system, for improving the passengers' on-board Wi-Fi experience [4]. However, the large coverage area of GEO satellites comes at the cost of high latency as well as substantial power loss. In particular, GEO satellites are at a distance of 35,768km, hence they suffer from a propagation delay of approximately 120 ms one-way delay from the ground to the satellite. Fortunately, the medium and low earth orbit (MEO/LEO) satellites are significantly closer to the earth, hence they have substantially lower latency compared to GEO satellites. More specifically, the LEO satellites at 300km are capable of offering the lowest latency of any of the satellite orbits at a propagation delay of 1 ms. However, the LEO satellites suffer from limited coverage and mobility, imposing different technical challenges from those of GEO satellites.

To circumvent the shortcomings of S2AC, DA2GC provides an alternative for providing low-latency, high-rate transmissions to aircraft [2]. The European Aviation Network (EAN) has been designed to deliver up to 75 Mbps per cell by combining an S-band satellite and the 4G LTE mobile terrestrial network [5]. However, the coverage area of DA2GC is limited, since the ground base stations (BSs) can only be deployed on dry land, while about $2/3$ of the earth's surface is covered by water. Furthermore, no ground BSs are available in remote airspaces, such as the polar regions, deserts, dense forests, etc. In this context, aeronautical *ad hoc* networking constitutes a promising technique of extending the DA2GC by enabling aircraft in the sky to act as relays for aiding data transmission [3], [6]. Furthermore, given the spherical nature of the globe, communications between two points is also limited by the direct line-of-sight visibility between the two points. As a result, the integration of A2AC with DA2GC and S2AC in aeronautical *ad hoc* networks (AANETs) becomes a promising solution for improving the in-flight connectivity via multi-hop communication techniques [7]. From a networking perspective, the objective of integrating A2AC with DA2GC is

This work would like to acknowledge the financial support of the Engineering and Physical Sciences Research Council projects EP/P034284/1 and EP/P003990/1 (COALESCE) as well as of the European Research Council's Advanced Fellow Grant QuantCom (Grant No. 789028).

J. Cui, D. Liu, S. Ng, Robert G Maunder and L. Hanzo are with the School of Electronics and Computer Science, University of Southampton, SO17 1BJ, Southampton (UK) (e-mail: {jingj.cui,d.liu}@soton.ac.uk and {sxn,rm,lh}@ecs.soton.ac.uk)).

J. Zhang is with Department of Computing & Informatics, Bournemouth University, BH12 5BB, U.K. (e-mail: jzhang3@bournemouth.ac.uk).

Halil Yetgin is with the Department of Electrical and Electronics Engineering, Bitlis Eren University, 13000 Bitlis, Turkey, and also with the Department of Communication Systems, Jozef Stefan Institute, SI-1000 Ljubljana, Slovenia (e-mail: hyetgin@beu.edu.tr).

to seamlessly convey long-distance tele-traffic from the ground BS to the destination aircraft by avoiding S2AC links, whilst maintaining reliable high-speed connections. Another potential benefit of AANETs relying on A2AC with DA2GC is that the integrated AANET becomes capable of reducing the latency as well as the spiralling communication cost of satellite providers.

In the integrated AANET, every entity including aircraft, satellites and ground BSs can act as relays for aiding transmission as part of the routing process. In contrast to the conventional mobile *ad hoc* networks (MANETs) or vehicular *ad hoc* networks (VANETs), the integrated AANET has its unique characteristics: 1) Different types of links exhibit different communication performance; 2) The movements of the nodes may be deemed sufficiently regular so that the network topology becomes predictable; 3) Aircraft travel at a high speed. Therefore, it is important to conceive and characterize routing strategies based on the network topology, whilst meeting diverse design goals [2], [6].

Numerous routing protocols have been designed for MANETs and VANETs in prior work [8]–[11]. In particular, routing protocols conceived for *ad hoc* networks can classified in different ways based on various characteristics. For instance, the family of proactive (table-driven) routing [12], reactive (on-demand) routing [13] and hybrid schemes [14] can be categorized based on their routing information update mechanism [8], [9]; Power-aware routing [15] and geographical information assisted routing [16] may be distinguished based on their specific resource utilization strategy [10]; Furthermore, unicast, multicast and broadcast routing are classified according to their particular communication patterns [11]. Indeed, several routing protocols may coexist within the same *ad hoc* network and may be activated based on specific situations. In [17], [18], simulation based comparisons of diverse routing techniques designed for MANETs having dynamically evolving network topologies have been investigated. Furthermore, an algorithm based on the combination of greedy forwarding and face routing[1] was proposed in [19] for achieving an asymptotically optimal solution. The concept of combining greedy forwarding and face routing was first introduced in [20] for avoiding falling dead ends during the greedy forwarding process, when routing in planer graphs. In [21], an improved greedy routing strategy relying on probabilistic neighbour selection was conceived for a context-aware MANET. The concepts of cognitive routing based on Q-learning was proposed for heterogeneous MANETs by appropriately selecting the transmission configuration in [22]. Numerous further routing protocols proposed for MANETs and VANETs can be found in [23]. However, given the unique heterogeneous nature and high mobility of the planes in AANETs, the existing routing solutions of MANETs and VANETs cannot be readily applied to large-scale integrated AANETs.

Hence bespoke routing designs have been conceived in [24]–[27] for AANETs relying on diverse performance metrics. More specially, in [24], a geographic load sharing based forwarding and handover strategy was proposed for airborne mesh networks relying on multi-server queueing models for striking a compelling balance between the capacity and the specific traffic load of each link. In [25], the characteristics of heterogeneous airborne networks relying on military radios were interpreted and their field tests complemented by a Request for Comment (RFC) 4938 (RFC4938) concerning their interaction with MANET protocols were reported on. Inspired by the accurate geographic information available for aircraft, a node trajectory density based routing algorithm was developed for maximizing the packet delivery probability in [26]. The application of forward error correction (FEC) schemes in AANETs was studied in [27], where a sophisticated data transfer protocol was proposed by combining fountain codes and the reliable user datagram protocol of [28]. As a further development, a coalitional game based framework was proposed for improving the spectrum efficiency relying on modelling the cognitive spectrum sensing and spectrum sharing between A2AC and DA2GC links of an aeronautical system [29]. The user association and resource allocation in an integrated satellite-drone network were studied in [30] by relying on a competitive market model. However, most of the research contributions found in the open literature were focused on finding the best route/resource allocation schemes based on simulated networks, rather than by considering the real flight data. Additionally, given the abundance of available spectrum in the millimetre-wave (mm-Wave) bands and the development of advanced large-scale antenna techniques, the application of mm-Wave communications for AANETs has attracted substantial attention from both academia and industry [31]–[33]. Consequently, we focus our attention on characterizing an integrated AANET operating in the mm-Wave frequency band. The historic evolution of AANETs is shown at a glance in Table. I.

TABLE I: Timeline of Routing Designs in AANETs.

2012	Geographic information assisted routing [24].
2013	Testing heterogeneous airborne networks relying on military radios [25] .
2014	AANET aided connectivity over the French sky and over the Atlantic ocean [6].
2016	Node trajectory density based routing algorithm [26] .
2018	The application of forward error correction (FEC) schemes in AANETs [27].
2019	The application of mm-Wave communications for AANETs [31].
2020	This work assessed routing algorithm with real aircraft data in North-Atlantic Region.

[1]Face routing walks along the line that connects the source and the destination, where face changes at the edges crossing the source-destination line.

Although various of routing algorithms haven been invoked for AANETs, there is a paucity of studies relying on real flight data. On the other hand, a key issue of routing in integrated AANETs is the link selection from the set of D2AC, S2AC and A2AC channels across the routes, whilst meeting the specific application-oriented performance. In this paper, we concentrate on a special class of routing problems – namely the shortest-path routing of integrated AANETs, which is synonymous with minimizing the total service delay subject to per-connection quality of service (QoS) constraints. The main contributions of the paper can be concluded as follows.

1) We investigate the QoS constrained delay minimization problem in the integrated AANET having aircraft, ground BS and satellites by selecting routes from D2AC, S2AC and A2AC links. Explicitly, we formulate a shortest-path routing problem between a dedicated pair of a ground BS and an aircraft with minimum-signal-to-noise ratio (SNR) constraints for each selected connection, which aims to extend the coverage of the ground BS by integrating DA2GC with A2AC and S2AC.
2) We employ a weighted directed graph (digraph) for modelling the integrated AANET with minimum-rate constraints and the curvature of the earth. As a result, the shortest-path routing problem formulated can be solved over the associated weighted digraph by invoking the shortest path algorithm based on the idea of Dijkstra's algorithm [34], which is capable of delivering the optimal solution.
3) We characterize our algorithm by harnessing three real flight datasets based on flights over the North-Atlantic oceanic area. In particular, our results reveal that the aircraft can be connected to the ground BS through AANETs between London Heathrow (LHR) Airport and New York's John F Kennedy (JFK) Airport. Furthermore, both our simulations and real flight-data driven results demonstrate that the A2AC links are capable of extending the DA2GC coverage with the aid of low-delay transmission.

The assumptions used in this paper are summarized as follows. In line with the studies [24], [35], [36], we assume that the integrated AANET is operated in half-duplex mode and the messages from different ground BSs are transmitted on different subchannels, hence resulting in no inter-link interference. Moreover, the system operates in the mm-Wave frequency band [31]–[33] and the channel between a pair of nodes is perfectly known at the transmitter [24], [31]. Therefore, the communication links in our AANET are assumed to benefit from a Line of Sight (LoS) propagation model [2], [37]. Additionally, we consider the system adopts the decode-and-forward protocol [38] and the end-to-end delay is measured by the sum of the transmission delay and propagation delay.

The rest of this paper is organized as follows. In Section II, the system model is presented, followed by the problem formulation of minimizing the total delay of the links selected for transmission in Section III. In Section IV, solutions for finding optimal routes are provided. Our simulation results are presented in Section V by relying on real flight data, followed by our conclusions in Section VI.

II. System model

A. System Description

We consider a ground-air-space integrated AANET comprising the ground layer, the aerial layer and the space layer of Fig. 1, where aircraft can be connected to certain ground BSs either via direct communication or by multi-hop communication techniques. In particular, the aircraft can build communication links with other aircraft, ground BSs and satellites via A2AC, DA2GC and S2AC techniques, respectively, in order to improve the on-board Internet experience of aircraft passengers. We assume that the integrated AANET considered is composed of N_1 aircraft, N_2 ground BS and N_3 satellites, where an example of the system model is illustrated in Fig. 1. Furthermore, given the mobility of aircraft during its flight its location changes rapidly. For clarity, we denote the entities in the system encompassing aircraft, ground BSs and satellites as a set of nodes $\mathcal{N} = \mathcal{N}_1 \cup \mathcal{N}_2 \cup \mathcal{N}_3$ with $N = |\mathcal{N}|$, where $\mathcal{N}_1 = \{1, \cdots, N_1\}$, $\mathcal{N}_2 = \{1, \cdots, N_2\}$ and $\mathcal{N}_3 = \{1, \cdots, N_3\}$. We assume that the integrated AANET is operated in half-duplex mode as in [36] and the messages from different ground BSs are transmitted on different subchannels resulting in no inter-link interference, representing an interference-free scenario. Table II provides a summary of the notations used in this paper.

Since aircraft typically fly 10km above the ground level, they benefit from negligible scatterers and shadowing effects. Hence we assume that the communication links in the AANET have LoS propagation [31], [32], [39], where the path-loss between node i and node j, $i, j \in \mathcal{N}$, can be expressed as

$$h_{i,j} = \left(\frac{c}{4\pi d_{i,j} f_c} \right)^{\alpha}, \tag{1}$$

where f_c is the carrier frequency and $c = 3 \times 10^8$ m/s is the speed of light. Furthermore, $d_{i,j}$ is the distance between node i as well as node j and α is the path-loss exponent.

B. Delay Model

In this paper, the delay model relies on the sum of the transmission and propagation delays of the individual connections. Moreover, we assume that the decode-and-forward (DF) relaying delay at each intermediate nodes is $D_{df} = 20$ ms.

Let us consider a communication link, where the message is sent from aircraft i to aircraft j. Hence the signal-to-noise ratio (SNR) at the receiver of aircraft j can be expressed as

$$\phi_{i,j} = \frac{P_i G_i^t G_j^r h_{i,j}}{\sigma^2}, \tag{2}$$

where σ^2 denotes the noise power. Furthermore, G_i^t and G_j^r are the transmit antenna gain and the receive antenna gain, respectively. Therefore, the data rate in the link spanning from node i to node j can be expressed as

$$C_{i,j} = B \log_2 \Big(1 + \phi_{i,j} \Big), \tag{3}$$

where B is the bandwidth allocated to the link. Correspondingly, given the size L of the data file to be transmitted in

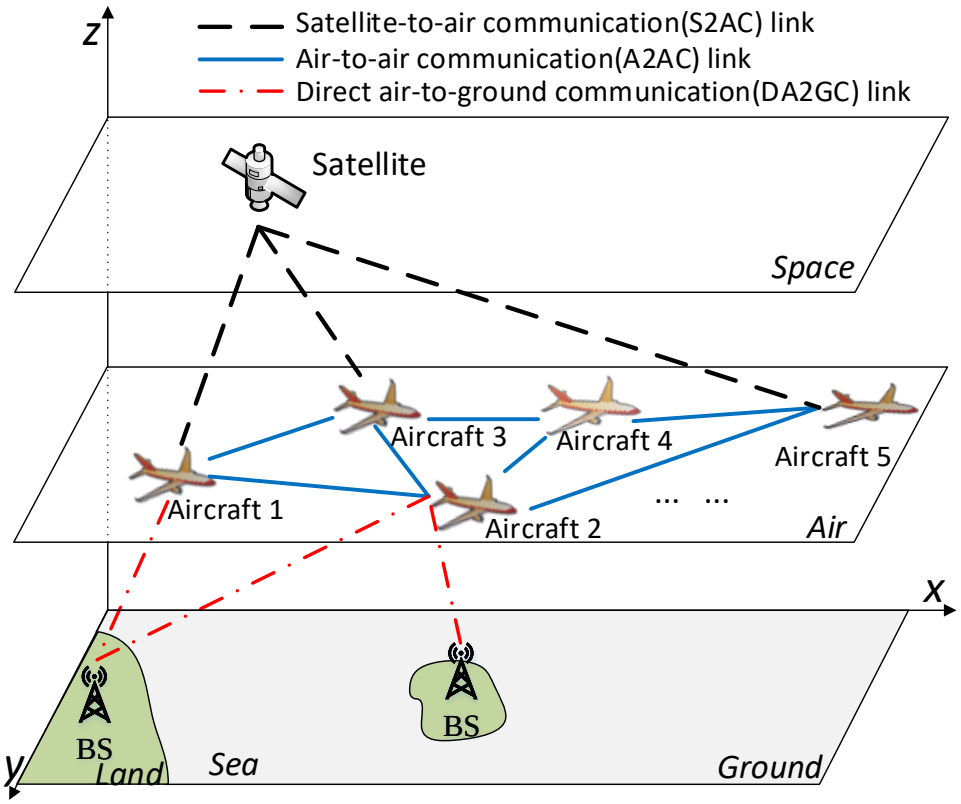

Fig. 1: Aircraft communication system by integrating ground and space communications.

TABLE II: The list of symbols and notations used in the paper.

Notation	Description	Notation	Description
$N, \mathcal{N}$	Number/set of total nodes	s,d	Source node and destination node
(i,j)	Link from node i to node j	ϕ_0	Predefined SNR threshold
$x_{i,j}$	Binary indicator of the link (i,j)	$\mathcal{X}$	Set of all possible $x_{i,j}$
$h_{i,j}$	Channel between node i and node j	d_{vis}	The greatest distance of two nodes that can be seen above the horizon
$f_c, c, d_{i,j}$ and α	Channel parameters	$d_{i,j}$	Distance between node i and node j
$\phi_{i,j}$	Received SNR at node j from node i	$\mathcal{G}$	Weighted digraph
P_i	Transmit power of node i	$\mathcal{V}$, $\mathcal{E}$	Set of nodes and edges in G, respectively
σ^2	Noise power	$\lvert\mathcal{Y}\rvert$	The cardinal number of set $\mathcal{Y}$
$G_i^t G_j^r$	Transmit/receive antenna gain	$e_{i,j}$	Edge in $\mathcal{G}$ corresponding to the link (i,j)
L	Size of data file to be transmitted	R^*, ψ^*	The optimal route and the corresponding minimum delay
$D_{i,j}$	Total delay from node i to node j	r, θ, φ	Parameters for a spherical coordinate system

bits, the file-transfer delay between node i and node j can be calculated as

$$D_{i,j}^{tr} = \frac{L}{C_{i,j}}. \tag{4}$$

The propagation delay is the time it takes for the signal to travel at the speed of light through the communication link from a node to the next one, which is given by

$$D_{i,j}^{pr} = \frac{d_{i,j}}{c}, \tag{5}$$

where $D_{i,j}^{pr} = D_{j,i}^{pr}$. As a result, the total delay from node i to node j can be expressed as

$$D_{i,j} = \begin{cases} D_{i,j}^{tr} + D_{i,j}^{pr}, & \text{if } j \text{ is the target aircraft,} \\ D_{i,j}^{tr} + D_{i,j}^{pr} + D_{df}, & \text{otherwise.} \end{cases} \tag{6}$$

III. Problem Formulation

Due to the curvature of the Earth, the maximum direct propagation distance between two aircraft is limited. Hence in addition to the QoS constraints, the communication between two nodes is also restricted by the radio-horizon, denoted as d_{vis}, which is relying on the height of the two nodes.

Our objective is to minimize the total delay of the links selected for transmission by appropriately selecting the routes between the source BS on the ground and the destination aircraft, which can be expressed as

$$\min_{x_{i,j} \in \mathcal{X}} \quad \sum_{i \in \mathcal{N}} \sum_{j \neq i, j \in \mathcal{N}} D_{i,j} x_{i,j} \tag{7a}$$

$$\text{s.t.} \quad x_{i,j} \phi_{i,j} \geq \phi_0, \ i \text{ is not the target aircraft,} \tag{7b}$$

$$d_{i,j} \leq d_{vis}, \tag{7c}$$

$$\sum_{\substack{j\neq i\\ j\in\mathcal{N}}} x_{i,j} - \sum_{\substack{j\neq i\\ j\in\mathcal{N}}} x_{j,i} = \begin{cases} 1, & \text{if } i = s, \\ -1, & \text{if } i = d, \\ 0, & \text{otherwise,} \end{cases} \tag{7d}$$

$$\sum_{j\neq i, j\in\mathcal{N}} x_{i,j} \begin{cases} \leq 1, & \text{if } i \neq d, \\ = 0, & \text{if } i = d, \end{cases} \tag{7e}$$

$$\forall i, j \in \mathcal{N}, i \neq j, \tag{7f}$$

where s and d denotes the source and the destination, respectively. $x_{i,j}$ is the link indicator function used, where we have $x_{i,j} = 1$ if link (i, j) is on the optimal route; Otherwise $x_{i,j} = 0$. Furthermore, ϕ_0 is a predefined SNR threshold to be exceeded for guaranteeing the received signal quality, while the constraints in (7b) and (7c) ensure that a communication link spanning from node i to node j exists. Specifically, (7b) guarantees that for link (i, j) the SNR at node j is higher than or equal to the predefined ϕ_0, while (7c) ensuring that node i and node j are visible above the horizon due to the curvature of the Earth. Finally, constraints in (7d) and (7e) ensure that the solution found from the problem formulated does indeed represent a legitimate path spanning from the ground BSs to the target aircraft.

Algorithm 1: Generated a weighted digraph based on the network information

Input : The dataset for the number and the locations of aircraft, ground BSs and Satellites.
Output: Generated weighted digraph of the AANET information
Init. : SNR threshold: ϕ_0; Values of system parameters: G^t, G^r, f_c and B;

repeat
  For $i \in \mathcal{N}$, calculate the received SNR at every other node j from node i using (2) denoted as $\boldsymbol{\phi}_i = \{\phi_{i,j},\ j \neq i \text{ and } j \in \mathcal{N}\}$;
  while $j \in \mathcal{N}$ *and* $j \neq i$ **do**
    if $\phi_{i,j} \geq \phi_0$ *and node* j *is visible to node* i **then**
      Calculate the delay based on (6) as the weight of the edge $e_{i,j}$;
      Add edge $e_{i,j}$ and its weight $D_{i,j}$ into the graph $\mathcal{G}$;
    end
  end
until *all nodes are visited*;

IV. Solutions for Finding Optimal Routes

As discussed in Section III, the delay minimization problem considered in this paper is an optimal route finding problem between the source node and the destination, which can be transformed into the optimal route-finding problem on a weighted digraph. Correspondingly, we first generate a weighted digraph based on the available network information by use of **Algorithm 1**, where the edges are generated based on the SNR constraints of (7b) and the constraints of the gretest horizon visible distance between two nodes of (7c). Then, we employ Dijkstra's algorithm for finding the optimal route of the problem in (7), which is described in **Algorithm 2**.

Specifically, the initialization process is given in **Algorithm 1**, in which a weighted digraph $\mathcal{G}(\mathcal{V}, \mathcal{E})$ is constructed based on the system information and the constraints of (7b) as well as (7c), where $\mathcal{V}$ and $\mathcal{E}$ represent the set of the nodes and the edges, respectively. Note that the initialization process in **Algorithm 1** is capable of reducing the size of the weighted digraph generated by removing the redundant edges and nodes by considering the constraints in (7b) and the curvature of the earth in (7c). As a result, we have $\mathcal{V} \subseteq \mathcal{N}$, since there are some isolated nodes that cannot connect to the graph $\mathcal{G}$. There are a number of approaches for finding the optimal route from the source to the destination such as Dijkstra's algorithm, dynamic programming as well as genetic algorithms. In this paper, we employ the best-first search strategy (also called priority-first search) of Dijkstra's algorithm for finding the optimal route of the problem in (7), which is summarized in **Algorithm 2** .

Explicitly, the ground BS and the target aircraft are defined to be the source and the destination node, respectively. The total delay between any two nodes is treated as the 'cost' of the link. In addition, the priority queue structure is used for storing the candidate nodes as well as the correlated cost information during the search process. The procedure of **Algorithm 2** starts by introducing a set $\psi = \{\psi_0, \cdots, \psi_N\}$ for storing the objective function (OF) values from the source node s to each of the other nodes during the search process. In ψ, all elements ψ_v, $v \in \mathcal{V}$, are initialized to ∞, except for $\psi_s = 0$. Furthermore, in **Algorithm 2**, the priority queue Q is used for storing the current leaves in the current search tree as well as their OF values in ψ, where the nodes in the priority queue Q are sorted in an ascending order based on the OF values. Specifically, the node having the minimum OF value has the top priority and thus will be first taken out. Moreover, $\mathrm{prev[v]} = u$ indicates that the parent of node v is u and thus the route spanning from s to d can be constructed by recursively visiting prev. To speed up the search process over the solution space, we introduce an additional variable ψ_{min} for storing the minimum delay spanning from the source node to the destination during the search process. Thus, ψ_{min} provides an upper bound of the OF value, since problem (7) is a minimization problem of the total delay. The step in line 11 guarantees that ψ_{min} is always the minimum OF value from s to d. Furthermore, $\hat{\psi}$ is an additional variable introduced for storing the temporary OF objective of the candidate path generated. Note that from the delay model of (6), the total delay spanning from the source node to any other node is monotonically increasing with the number of nodes in the route. As a consequence, the leaf node v in Q associated with $\psi_v > \psi$ will be pruned as seen in line 18, which is capable of significantly reducing the search space, especially for large networks. However, in the worst-case scenario, **Algorithm 2** will have the same complexity as the standard Dijkstra algorithm [40], which is of the order of $\mathcal{O}(|\mathcal{E}| + |\mathcal{V}| \log |\mathcal{V}|)$.

Algorithm 2: The shortest-path routing algorithm

Input : Weighted digraph of AANETs obtained from **Algorithm 1**; The start node s and the destination d;

Output: The optimal route R^* and the minimum delay ψ^*;

Init. : A priority queue $Q = \emptyset$;

Initialize $\psi = \{\psi_v, \forall v \in \mathcal{V}\}$, where $\psi_v = 0$ if v is s, and $\psi_v = \inf$ if otherwise. Set $\psi_{min} = \inf$;

Push ψ_s and s to Q;

while Q *is not empty* **do**

  Pop the vertex u and ϕ_u;

  if $u = d$ **then**

    $\phi_{min} = \min\{\phi_{min}, \phi_u\}$;

  end

  while v *is a neighbor of* u **do**

    $\hat{\psi} = \psi_u + D_{u,v}$;

    if $\psi_v >= \hat{\psi}$ *and* $\psi_v \leq \psi_{min}$ **then**

      $\psi_v = \hat{\psi}$; $\text{prev}[v] = u$;

      Store ψ_v and v into the Q;

    end

  end

end

Constitute R from prev; $\psi^* = \psi_d$ and $R^* = R$;

V. Simulations

In this section, we evaluate the performance of the proposed algorithms by computer simulations. We first investigate the results based on simulations in Section V-A. Then we apply our algorithms to real flight datasets collected in the North-Atlantic region in Section V-B for validating the performance of the algorithms, which also reveals the potential benefits of AANETs in terms of improved connectivity.

A. Numerical Results

To model flight paths and the satellite orbits above the Earth surface, the spherical coordinate system denoted by (r, θ, φ) is considered, where the origin is located in the center of the earth. Furthermore, r is the distance of a point from the origin, while θ and φ are the polar angle and the azimuthal angle of the point, respectively. Fig. 2 illustrates an example of the spherical coordinate system used, where r_{earth} is the radius of the earth. Hence, the distance between the origin O and node i is $r_i = H_i + r_{earth}$. As a result, the locations of aircraft, the ground BS and satellites can be denoted as $(r_i, \theta_i, \varphi_i)$, $i \in \mathcal{N}$. To characterise the proposed algorithm, we first consider the simple scenario of $N_2 = N_3 = 1$. Without loss of generality, we treat the ground BS as the reference point of the system in the spherical coordinate system, i.e., $\theta_s = \varphi_s = 0$. The target aircraft is located at the point $\theta_d = \frac{\pi}{4}$ and $\varphi_d = \frac{\pi}{6}$, while the GEO satellite is located at the center of the region with $\theta_s = \frac{\pi}{8}$ and $\varphi_s = \frac{\pi}{12}$. Furthermore, the values of θ_a and φ_a for the intermetiate aircraft are randomly drawn from a uniform distribution with $\theta_a \in [0, \theta_d]$ and $\phi_a \in [0, \varphi_d]$, respectively. Hence, all figures are plotted over 1000 realizations. Note that

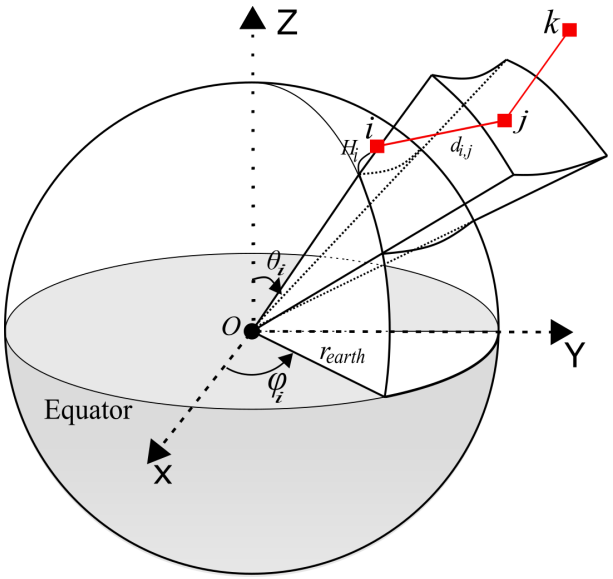

Fig. 2: Illustration of the spherical coordinate system, where three nodes i, j and k are located above the earth with different altitudes.

the distance between the ground BS and the target aircraft is about 3300 km, and thus the ground BS cannot communicate directly with the target aircraft due to the curvature of the Earth. Moreover, we assume that the system operates at the mm-Wave frequency of $f_c = 31$ GHz and the noise power is $\sigma^2 = -132$ dBm [31]. The other parameters used in our simulations are the same as those in [39]. Specifically, the transmit powers of the ground BS, of the aircraft and of the satellite are 45dBm, 30dBm and 50dBm, respectively. Furthermore, we have $G_i^t = G_i^r = 25$dB for the ground BS and the aircraft, while $G_i^t = G_i^r = 45$dB for the satellite along with $B = 200$MHz and $\phi_0 = 0$dB. The heights of the ground BS, the aircraft as well as the satellite are 50m,10.7 km and 35768 km, respectively. In particular, the greatest distance between two points i and j above the horizon is calculated by $d_{vis} < 3.57(\sqrt{H_i} + \sqrt{H_j})$, where d_{vis} is in kilometers and H_i and H_j are in meters.

Fig. 3 illustrates the total delay and the number of hops in the shortest path[2] versus the number of intermediate relaying aircraft with different schemes, where the transport block size of $L = 9000$ bits is used as in [41]. For comparisons, we consider two different schemes. In Scheme 1, we assume that the ground BS is able to communicate with the target aircraft via A2AC links, which provides a lower bound of the end-to-end delay. Note that the distance between the ground BS and the target aircraft is around 3300 km in the model considered, hence it requires six hops at least due to the constraint of the visible distance. As a result, the lowest possible delay can be attained according to (6). In Scheme 2, we consider satellite aided communications, which only has two hops due to the large coverage area of the GEO satellite. Therefore, Fig. 3(a) illustrates how the total delay and the number of hops in the shortest path vary upon increasing the number

[2]Note that in this paper the number of hops in a path denotes the number of edges nodes in the path. For instance, consider a route with four nodes like $s \to n_1 \to n_2 \to d$, the number of hops is 3.

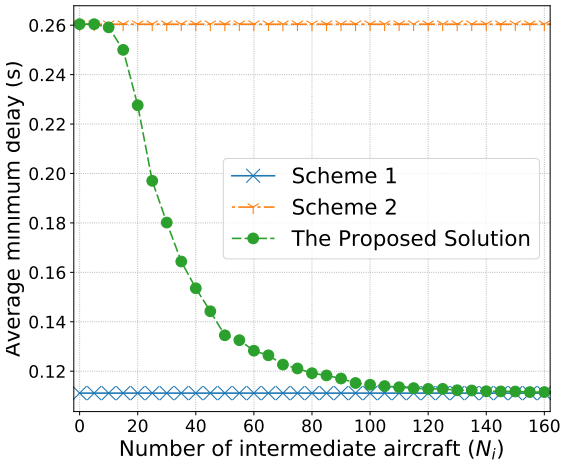

(a) Delay versus the number of the intermediate aircraft.

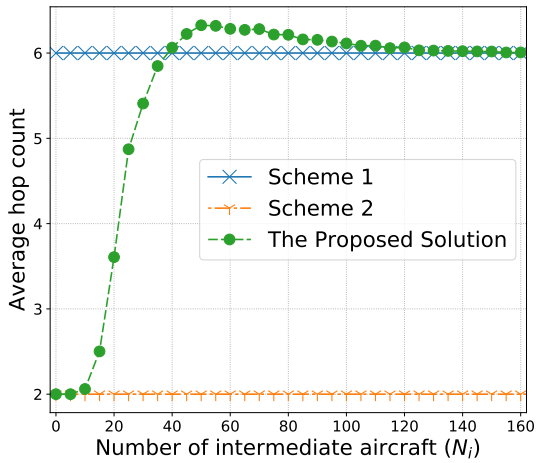

(b) Hop counts versus the number of the intermediate aircraft.

Fig. 3: Comparisons of the total delay as well as the hop count for three different schemes.

N_i of intermediate aircraft. As seen from Fig. 3(a), the total delay of the proposed solution is substantially reduced upon increasing the number of intermediate aircraft. In particular, the minimum delay attained by the proposed algorithm closely approaches the lower bound of Scheme 1, when $N_i \geq 120$. This indicates that aircraft aided multi-hop communications substantially reduces the end-to-end delay upon using the proposed algorithm. As observed from Fig. 3(b), the hop count of the proposed solution is lower than that of Scheme 1 when $N_i < 35$ owing to occasionally opting for the satellite link as part of the shortest path for avoiding any potential route breakage. However, the hop count becomes higher than that of Scheme 1 when $N_i \leq 40$. Furthermore, the hop count of the proposed solution closely approaches that of Scheme 1 when $N_i \leq 120$ as in Fig. 3(a), which implies that the hop count in the proposed solution approaches the minimum number of hops required, when the number of intermediate aircraft is high enough. Fig. 4 illustrates the impact of the file size on the total delay. As seen from Fig. 4, the total delay between the source on the ground and the target aircraft is reduced upon increasing the number of aircraft, because this improves the probability of selecting a lower-delay aircraft-aided multi-hop link instead of the two-hop, yet high-delay satellite link for reaching the target aircraft. Therefore, when there is a shortage of intermediate aircraft, the ground BS communicates with the target aircraft via the satellite, which results in a higher propagation delay compared to A2AC links. In this context, the total propagation delay is dominated by that of the satellite links. Hence the delay versus N_i curve of Fig. 4 remains relatively flat when the number of aircraft is below about 20. Furthermore, we can observe that upon increasing the file size of L from 1Mbit to 9Mbit, the delay difference between $N_i = 0$ and $N_i = 100$ is substantially increased. This is mainly due to the large altitude footprint requiring less hops required in the satellite aided transmission than in the A2AC aided transmission. As a consequence, there is a tradeoff between the satellite aided transmission and the A2AC aided transmission.

Let us elaborate briefly on a simple scenario with all links having an equal transmission rate of $C = 10$Mbps. For the satellite aided transmission, the total uplink and downlink propagation delay is about $D_{pr} = 240$ms, while the total uplink plus downlink file-transfer delay is $D_{tr} = 40$ms for a $L = 200$Kbit file. Finally, the DF relaying delay is assumed to be $D_{df} = 20$ms. Thus, we can obtain the total delay of $D^{S2AC} = 300$ms for an $L = 100$Kbit file. By contrast, for the A2AC aided transmission relying on five hops in Scheme 1, the total propagation delay is around $D_{pr} = 11$ ms for a distance of 3300km, the file-transfer delay is $D_{tr} = 120$ms and $D_{df} = 100$ms. Hence, we have the total delay of $D^{A2AC} = 231$ms. In this case, the A2AC aided transmission outperforms the satellite aided transmission. On the other hand, when the ground BS has an $L = 1$Mbit file for transmission, we have $D^{S2AC} = 460$ms while $D^{A2AC} = 711$ms, which results in a lower delay upon using the satellite than using the A2AC link[3]. This reveals that aircraft aided multi-hop communications may have an advantage in providing lower-delay services than satellite aided communications, provided that the file is not excessively large.

B. Flight Data Driven Results

In this subsection, we characterize the system performance for the five busiest TransAtlantic airlines using real historical flight data collected over the North-Atlantic region, which includes Delta Airline, United Airline, American Airline, British Airways and Lufthansa. Specifically, these datasets contain the historical flight information of the area recorded at sampling intervals of 10s, where each entry of the flight contains the following information: timestamp, longitude, latitude, altitude and speed. The data in the first and second datasets are collected from 00:00 on 24 Dec. 2017 until 00:00 on 26 Dec.2017, which is typically the quietest day of the year. The

[3]Note that given a transmission rate C, there is a threshold L_{th}, where the A2AC aided transmission is beneficial if $L < L_{th}$, otherwise the satellite aided transmission has a lower delay. In particular, from the delay model of (6), we have $L_{th} \approx \frac{3.658C}{100}$

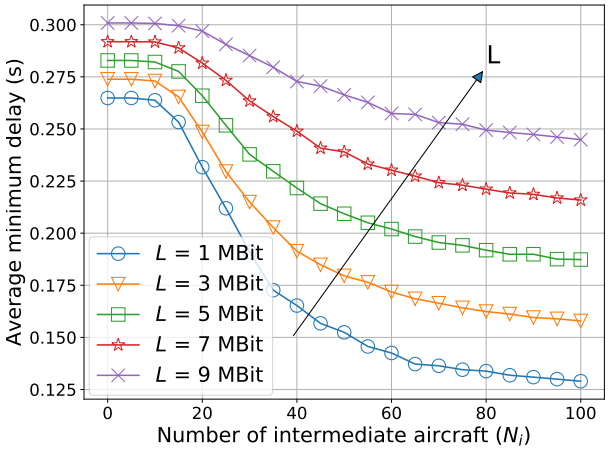

Fig. 4: The impact of file size on the minimum delay.

first dataset, referred to as Data-1, contains the TransAtlantic flights between LHR Airport and JFK Airport as in the previous example, which consists of 57 flights and 17,281 entries for each flight. The second dataset, referred as Data-2, contains all TransAtlantic flights of the 5 busiest TransAtlantic airlines, which consists of 381 flights and 17,281 entries for each flight. The data in the third dataset were collected from 00:00 on 29 Jun. 2018 to 00:00 on 30 Jun. 2018, which is the busiest day of the year having the most flights. Similar to the scenario of Data-2, the third dataset, Data-3, contains 649 flights and 8,641 entries for each flight. Moreover, the file size used is $L = 200$Kbit and all the other parameters used in our simulations are the same as in Section V-A.

Fig. 5 shows an example topology of the AANET attained from Data-2 and Data-3 as well as the shortest paths found from the ground BS at LHR to BA117, when the flight distance of BA117 is 3532 km and each link has a fixed file-transfer rate $C = 10$Mbps. In Fig. 5, the stars denote LHR (the ground BS) and JFK, while green circles denote the planes in the network. Furthermore, the red dashed lines denote the shortest path to BA117 (the square) and the triangles are the intermediate planes. As seen from Fig. 5(a), the shortest path from the ground BS at LHR to BA117 in Data-2 has seven hops (Ground BS→DL229→AA151→UA53→DL231→BA195→ DL83 →BA117) and its delay is 272.46ms, while the shortest path found for BA117 in Data-3 has six hops (GroundBS→UA988→UA24 →DL177→AA25→ AA725 →BA117) and its delay is 231.75ms in Fig. 5(b). We can see that both the delay and the hop count of the shortest path found for Data-3 is lower than that for Data-2, which confirms that the AANET has lower delay during the busiest day than that in the quietest day of the year. This is owing to the fact that there are more flights in Data-3 than in Data-2, since having more planes available approaches the ideal scenario of Scheme 1.

Fig. 6 shows the cumulative degree distribution (CDD) of the connected graph modelling different networks generated from the three datasets for providing us with a glimpse into the structure of a network, where the CDD represents the specific fraction of nodes having a degree smaller than a given number k on the abscissa axis. We observe that there are many nodes with degree zero for Data-1, which implies that there is no communication link between the ground BS at LHR and BA117. Furthermore, we can see that the probability of the nodes with the degree of $k \geq 12$ is about 20% for Data-2, while it is higher than 40% for Data-3. Moreover, the maximum degree of a node in Fig. 6 for Data-3 is 276, while it is 160 for Data-2 and 12 for Data-1, respectively.

Fig. 7 shows the cumulative distribution functions (CDFs) of both the hop count and of the total delay of the shortest paths found during the period of the complete travel of BA117 from LHR to JFK. Explicitly, Fig. 7(a) and Fig. 7(b) shows the cumulative probability distributions of the hop count and the total delay in the shortest paths found in the three datasets throughout the complete travel of BA117. It can be observed from the delay model of (6) that the total delay of a route relies on the number of hops. As a result, the CDF curves of the hop count have the similar trends as those of the total delay in terms of the shortest paths found. Furthermore, Fig. 7 also illustrates that both the hop count and the delay attained from Data-3 are more beneficial than those of Data-2 and Data-1, since there are more available flights in Data-3. More specifically, observe from Fig. 7 that during the complete period of travel there is a low success probability of around 30% for BA117 to communicate with the ground BS via AANETs for Data-1. By contrast, for Data-2 and Data-3, BA117 is capable of connecting to the ground BS via multi-hop communications during its complete travel.

VI. Conclusions

In this paper, we investigated the routing problem of AANET-assisted integrated ground-air-space communications with the objective of providing in-flight connectivity. Whilst relying both on aircraft and ground BSs as well as satellites, we minimized the total delay by considering the propagation delay, file-transfer delay and DF relaying delay. Furthermore, we have developed a weighted digraph for modelling the integrated AANET under minimum-rate constraints for finding the optimal route. Both the simulation results and real historical flight data driven results revealed that the AANET-aided transmission has the potential benefit of extending the DA2GC coverage while providing reduced-delay transmissions. A promising extension of this research is to consider the multi-component Pareto-optimization of AANET-assisted integrated networks for striking a compelling tradeoff amongst different performance metrics such as the delay, the energy efficiency as well as spectral efficiency, just to name a few.

References

[1] (2019) Global Market Forecast. [Online]. Available: https://www.airbus.com/aircraft/market/global-market-forecast.html

[2] M. Vondra, E. Dinc, M. Prytz, M. Frodigh, D. Schupke, M. Nilson, S. Hofmann, and C. Cavdar, "Performance study on seamless DA2GC for aircraft passengers toward 5G," *IEEE Commun. Mag.*, vol. 55, no. 11, pp. 194–201, Nov. 2017.

[3] J. Zhang, T. Chen, S. Zhong, J. Wang, W. Zhang, X. Zuo, R. G. Maunder, and L. Hanzo, "Aeronautical *ad hoc* networking for the Internet-above-the-clouds," *Proc. IEEE*, vol. 107, no. 5, pp. 868–911, May 2019.

[4] Gogo-blog. (2019) Gogo Reaches Approximately 1,300 Commercial Aircraft Installed with Satellite IFC Technology. [Online]. Available: https://concourse.gogoair.com/

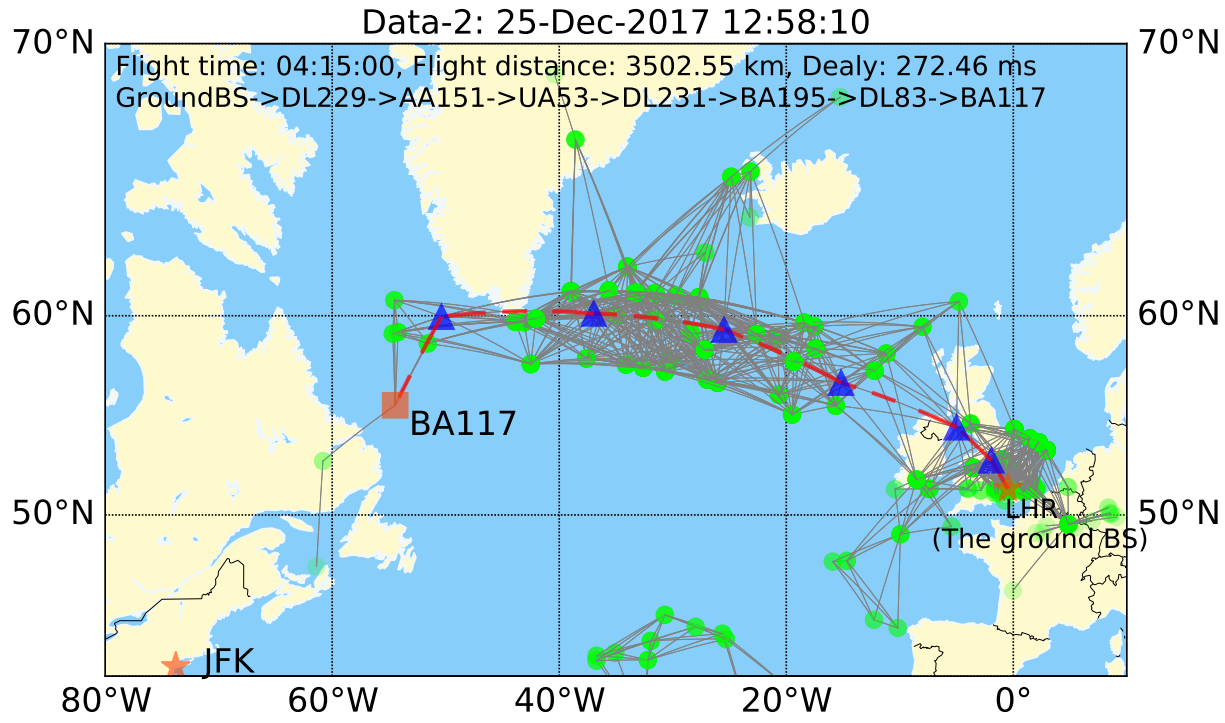

(a) Results on Data-2

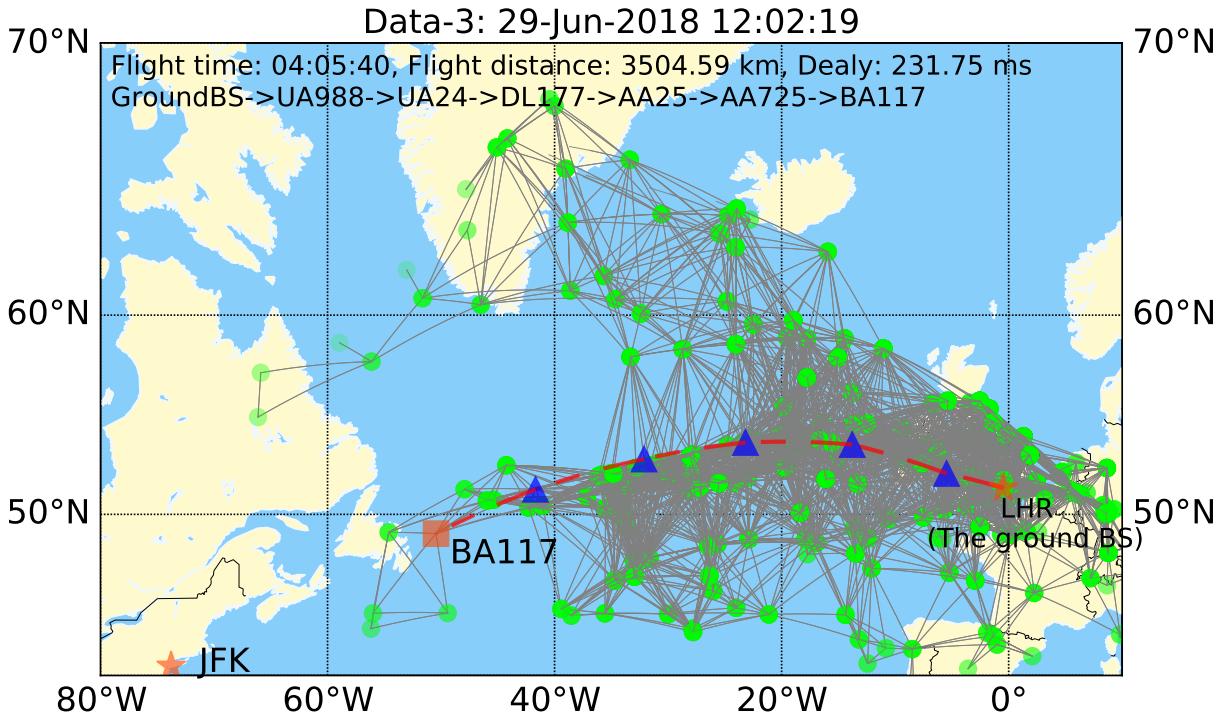

(b) Results on Data-3

Fig. 5: Comparisons of BA117 in AANETs over different datasets.

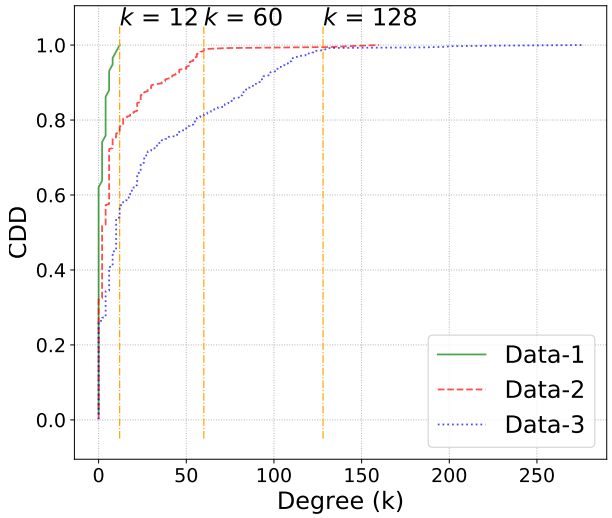

Fig. 6: Degree distribution of AANET with different datasets.

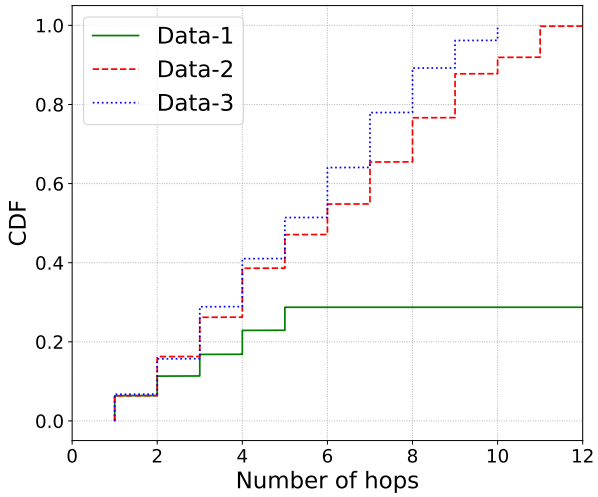

(a) CDFs of hops in the shortest paths

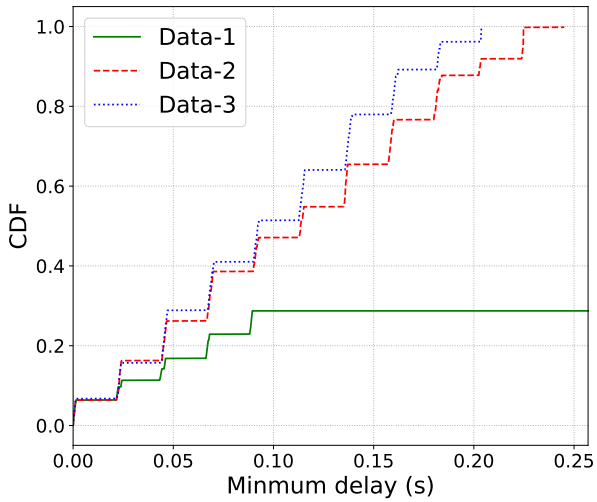

(b) CDFs of the delay in the shortest paths

Fig. 7: CDFs of hops and the total delay of the shortest paths found by the proposed algorithm.

[5] (2015, Sep.) The European aviation network. [Online]. Available: https://www.telekom.com/resource/blob/390304/.../dl-150929-datenblatt-data.pdf

[6] Q. Vey, A. Pirovano, J. Radzik, and F. Garcia, "Aeronautical *ad hoc* network for civil aviation," in *Communication Technologies for Vehicles*, A. Sikora, M. Berbineau, A. Vinel, M. Jonsson, A. Pirovano, and M. Aguado, Eds. Cham: Springer International Publishing, 2014, pp. 81–93.

[7] F. Hoffmann, D. Medina, and A. Wolisz, "Joint routing and scheduling in mobile aeronautical *ad hoc* networks," *IEEE Trans. Veh. Technol.*, vol. 62, no. 6, pp. 2700–2712, Jul. 2013.

[8] M. K. Marina and S. R. Das, "On-demand multipath distance vector routing in *ad hoc* networks," in *Proc. Int. Conf. Network Protocols (ICNP)*, Nov 2001, pp. 14–23.

[9] M. Abolhasan, T. Wysocki, and E. Dutkiewicz, "A review of routing protocols for mobile *ad hoc* networks," *Ad Hoc Networks*, vol. 2, no. 1, pp. 1 – 22, 2004. [Online]. Available: http://www.sciencedirect.com/science/article/pii/S157087050300043X

[10] A. D. Devangavi and R. Gupta, "Routing protocols in VANET — A survey," in *Int. Conf. Smart Tech. For Smart Nation (SmartTechCon)*, Aug 2017, pp. 163–167.

[11] P. K. McKinley, H. Xu, A. . Esfahanian, and L. M. Ni, "Unicast-based multicast communication in wormhole-routed networks," *IEEE Trans. Parallel Distrib. Syst.*, vol. 5, no. 12, pp. 1252–1265, Dec 1994.

[12] P. Jacquet, P. Muhlethaler, T. Clausen, A. Laouiti, A. Qayyum, and L. Viennot, "Optimized link state routing protocol for *ad hoc* networks," in *Proc. of IEEE Int. Multi Topic Conf. (INMIC). Technology for the 21st Century.*, Dec 2001, pp. 62–68.

[13] C. E. Perkins and E. M. Royer, "*Ad-hoc* on-demand distance vector routing," in *Proc. of IEEE Workshop Mob. Comput. Syst. and Applications (WMCSA)*, Feb 1999, pp. 90–100.

[14] Z. J. Haas and M. R. Pearlman, "The performance of query control schemes for the zone routing protocol," *IEEE/ACM Trans. Netw.*, vol. 9, no. 4, pp. 427–438, Aug 2001.

[15] S. Singh, M. Woo, and C. S. Raghavendra, "Power-aware routing in mobile *ad hoc* networks," in *Proc. of 4th Annual ACM/IEEE Int. Conf. Mobile Computing Networking (MobiCom)*. New York, NY, USA: Association for Computing Machinery, Oct. 1998, p. 181–190. [Online]. Available: https://doi.org/10.1145/288235.288286

[16] Y. Yu, R. Govindan, and D. Estrin, "Geographical and energy aware routing: a recursive data dissemination protocol for wireless sensor networks," Tech. Rep., 2001.

[17] D. A. Maltz, J. Broch, D. Johnson, Y.-C. Hu, and J. Jetcheva, "A performance comparison of multi-hop wireless *ad hoc* network routing protocols," in *Proc. ACM MobiCom*, vol. 114, 1998, pp. 85–97.

[18] C. Mbarushimana and A. Shahrabi, "Comparative study of reactive and proactive routing protocols performance in mobile *ad hoc* networks," in *21st International Conference on Advanced Information Networking and Applications Workshops (AINAW'07)*, vol. 2, May 2007, pp. 679–684.

[19] F. Kuhn, R. Wattenhofer, and A. Zollinger, "An algorithmic approach to geographic routing in *ad hoc* and sensor networks," *IEEE/ACM Trans. Netw.*, vol. 16, no. 1, pp. 51–62, Feb. 2008.

[20] E. Kranakis, H. Singh, and J. Urrutia, "Compass routing on geometric networks," in *IN PROC. 11 TH CANADIAN CONFERENCE ON COMPUTATIONAL GEOMETRY*, 1999, pp. 51–54.

[21] P. K. Biswas, S. J. Mackey, D. H. Cansever, M. P. Patel, and F. B. Panettieri, "Context-aware smallworld routing for wireless $ad-hoc$ networks," *IEEE Trans. Commun.*, vol. 66, no. 9, pp. 3943–3958, Sep. 2018.

[22] A. Al-Saadi, R. Setchi, Y. Hicks, and S. M. Allen, "Routing protocol for heterogeneous wireless mesh networks," *IEEE Trans. Veh. Technol.*, vol. 65, no. 12, pp. 9773–9786, Dec 2016.

[23] F. Cadger, K. Curran, J. Santos, and S. Moffett, "A survey of geographical routing in wireless Ad-Hoc networks," *IEEE Commun. Surveys Tuts.*, vol. 15, no. 2, pp. 621–653, Second 2013.

[24] D. Medina, F. Hoffmann, F. Rossetto, and C. Rokitansky, "A geographic routing strategy for North Atlantic in-flight Internet access via airborne mesh networking," *IEEE/ACM Trans. Netw.*, vol. 20, no. 4, pp. 1231–1244, Aug. 2012.

[25] B. Cheng, A. Coyle, S. McGarry, I. Pedan, L. Veytser, and J. Wheeler, "Characterizing routing with radio-to-router information in a heterogeneous airborne network," vol. 12, no. 8, pp. 4183–4195, Aug. 2013.

[26] Q. Vey, S. Puechmorel, A. Pirovano, and J. Radzik, "Routing in aeronautical *ad-hoc* networks," in *IEEE/AIAA Digital Avionics Systems Conference (DASC)*, Sep. 2016, pp. 1–10.

[27] Q. Luo and J. Wang, "FRUDP: A reliable data transport protocol for aeronautical $ad\ hoc$ networks," *IEEE J. Sel. Areas Commun.*, vol. 36, no. 2, pp. 257–267, Feb. 2018.

[28] T. Bova and T. Krivoruchka, " RELIABLE UDP PROTOCOL," Feb. 1999, draft-ietf-sigtran-reliable-udp-00.txt.

[29] B. Du, R. Xue, L. Zhao, and V. C. M. Leung, "Coalitional graph game for air-to-air and air-to-ground cognitive spectrum sharing," *IEEE Trans. Aerosp. Electron. Syst.*, pp. 1–1, 2019.

[30] Y. Hu, M. Chen, and W. Saad, "Joint access and backhaul resource management in satellite-drone networks: A competitive market approach," *IEEE Trans. Wireless Commun.*, vol. 19, no. 6, pp. 3908–3923, 2020.

[31] S. Hofmann, A. E. Garcıa, D. Schupke, H. E. Gonzalez, and F. H. Fitzek, "Connectivity in the air: Throughput analysis of air-to-ground systems," in *IEEE Proc. of International Commun. Conf. (ICC)*, May 2019, pp. 1–8.

[32] T. Cuvelier and R. W. Heath, "Mmwave MU-MIMO for aerial networks," in *Int. Symp. Wireless Commun. Sys. (ISWCS)*, Aug. 2018, pp. 1–6.

[33] X. Huang, J. A. Zhang, R. P. Liu, Y. J. Guo, and L. Hanzo, "Airplane-aided integrated networking for 6G wireless: Will it work?" *IEEE Veh. Technol. Mag.*, vol. 14, no. 3, pp. 84–91, Sep. 2019.

[34] E. W. Dijkstra, "A note on two problems in connexion with graphs," *Numerische Mathematik*, vol. 1, no. 1, pp. 269–271, Dec 1959. [Online]. Available: https://doi.org/10.1007/BF01386390

[35] Q. Vey, A. Pirovano, J. Radzik, and F. Garcia, "Aeronautical ad hoc network for civil aviation," in *Communication Technologies for Vehicles*, A. Sikora, M. Berbineau, A. Vinel, M. Jonsson, A. Pirovano, and M. Aguado, Eds. Cham: Springer International Publishing, 2014, pp. 81–93.

[36] T. Z. H. Ernest, A. S. Madhukumar, R. P. Sirigina, and A. K. Krishna, "Outage analysis and finite SNR diversity-multiplexing tradeoff of hybrid-duplex systems for aeronautical communications," *IEEE Trans. Wireless Commun.*, vol. 18, no. 4, pp. 2299–2313, Apr. 2019.

[37] E. Lagunas, S. K. Sharma, S. Maleki, S. Chatzinotas, and B. Ottersten, "Resource allocation for cognitive satellite communications with incumbent terrestrial networks," *IEEE Trans. Cog. Commun. Netw.*, vol. 1, no. 3, pp. 305–317, Sep. 2015.

[38] C. Bae and W. E. Stark, "End-to-end energy–bandwidth tradeoff in multihop wireless networks," *IEEE Trans. Inf. Theory*, vol. 55, no. 9, pp. 4051–4066, Sep. 2009.

[39] M. Vondra, M. Ozger, D. Schupke, and C. Cavdar, "Integration of satellite and aerial communications for heterogeneous flying vehicles," *IEEE Network*, vol. 32, no. 5, pp. 62–69, Sep. 2018.

[40] M. L. Fredman and R. E. Tarjan, "Fibonacci heaps and their uses in improved network optimization algorithms," *J. ACM*, vol. 34, no. 3, p. 596–615, Jul. 1987. [Online]. Available: https://doi.org/10.1145/28869.28874

[41] 3GPP, "5G NR: Packet Data Convergence Protocol (PDCP) specification," *3GPP TS 38.323*, vol. version 15.2.0 Release 15, Sep. 2018.